J. Fluid Mech. (1969), *vol.* 39, *part* 3, *pp.* 477–495
Printed in Great Britain

Growth of fingers at an unstable diffusing interface in a porous medium or Hele–Shaw cell

By R. A. WOODING
C.S.I.R.O. Division of Plant Industry, Canberra, A.C.T., Australia

(Received 17 April 1969)

Waves at an unstable horizontal interface between two fluids moving vertically through a saturated porous medium are observed to grow rapidly to become fingers (i.e. the amplitude greatly exceeds the wavelength). For a diffusing interface, in experiments using a Hele–Shaw cell, the mean amplitude taken over many fingers grows approximately as (time)^2, followed by a transition to a growth proportional to time. Correspondingly, the mean wave-number decreases approximately as (time)$^{-\frac{1}{2}}$. Because of the rapid increase in amplitude, longitudinal dispersion ultimately becomes negligible relative to wave growth. To represent the observed quantities at large time, the transport equation is suitably weighted and averaged over the horizontal plane. Hyperbolic equations result, and the ascending and descending zones containing the fronts of the fingers are replaced by discontinuities. These averaged equations form an unclosed set, but closure is achieved by assuming a law for the mean wave-number based on similarity. It is found that the mean amplitude is fairly insensitive to changes in wave-number. Numerical solutions of the averaged equations give more detailed information about the growth behaviour, in excellent agreement with the similarity results and with the Hele–Shaw experiments.

1. Introduction

Although flows in porous media generally involve extremely low Reynolds numbers (the so-called Darcy flows), the existence of several mechanisms which could induce instability has been recognized for many years (Horton & Rogers 1945; Lapwood 1948; Saffman & Taylor 1958). In particular, most of these effects can appear at an interface between two fluids in a porous medium.

Saffman & Taylor pointed out that the instability which may arise at a moving interface between two immiscible fluids in a porous medium possesses analogies to Taylor instability (Taylor 1950). They considered a small perturbation (of wave-number α) to a horizontal interface, when the steady state was one of uniform fluid velocity W upwards, and showed that the initial growth law was proportional to $\exp(2\Lambda^*\alpha T)$. Here T is time and

$$2\Lambda^*\left(\frac{\mu_1}{k_1}+\frac{\mu_2}{k_2}\right) = g(\rho_1-\rho_2)+\left(\frac{\mu_1}{k_1}-\frac{\mu_2}{k_2}\right)W, \tag{1}$$

in which ρ and μ refer to the fluid density and viscosity, while k denotes perme-

ability of the medium and g denotes gravity. The suffixes $_1$ and $_2$ refer to the upper and lower fluids respectively.

In an extension of their work, Saffman & Taylor treated the growth of large-amplitude waves, or 'fingers', at the interface between immiscible fluids in a Hele–Shaw cell. At large times the amplitude, measured from the centre of a finger, tends to $\Lambda^* T$, and the flow within the finger is uniform.

When the interface is formed between two fluids which can inter-diffuse, there still exists a characteristic dimension ΛT, where Λ is a velocity analogous to Λ^*. A second characteristic dimension is the growing thickness $(\kappa T)^{\frac{1}{2}}$ of the interface, where κ is an appropriate diffusivity. Elimination of T between these two quantities gives the 'natural' length scale κ/Λ (cf. Foster 1968.)

For the instability problem, Elder (1968) observed that there were analogies with both Taylor and Rayleigh instability mechanisms, and suggested that the most rapidly amplified waves involved wavelengths comparable with the thickness of the diffusion layer. (See also Heller 1966).

Elder carried out numerical experiments on the early growth of instabilities at various types of thermal interface, including the sublayer at a heated horizontal boundary within a porous medium. The latter case is assumed here to be qualitatively applicable to the free interface in a porous medium, and the main results may be summarized briefly as follows. (i) After a rapid initial development, a small almost-steady induced flow exists due to thermal 'noise' already present in the system. (ii) In the next stage the growth of the disturbance is closely exponential, with exponent proportional to the square of the Rayleigh number. It can be shown from this growth law that the disturbance wave-number is scaled as Λ/κ. In this régime the amplitude increases by at least one order of magnitude. (iii) The system changes to one of approximately constant acceleration, with displacements, presumably, increasing as the square of the time. A further order-of-magnitude increase in amplitude occurs, the disturbance attaining a magnitude of at least $O(1)$; thus this régime is distinctly non-linear and the form of the sublayer is considerably modified.

In Elder's view, the acceleration arises because progressively more buoyant fluid from deeper inside the sublayer is drawn into the disturbance (which now resembles a series of 'blobs'), thus increasing the effective density difference. This process continues until the sublayer is largely removed.

Elder's numerical results are particularly valuable because they cover a range which is extremely difficult to observe experimentally. By comparison, the behaviour of large-amplitude waves, or fingers, is easy to observe, but may be difficult to treat numerically. This paper is concerned with the latter system at an unstable free interface in a porous medium. It should be noted that the study does not lead to a fully determinate model, since the initial-value problem is not treated here, but amplitude–wave-number relationships can be found.

The equations of the flow

For flows of inhomogeneous fluids at very low Reynolds numbers (defined relative to the pore diameter) in a porous medium, the appropriate general equations are given below.

Continuity:
$$\nabla . \mathbf{q} = 0, \tag{2}$$

where $\mathbf{q}$ is the volume flow vector.

Darcy's law:
$$\nabla P - \rho \mathbf{g} + \frac{\mu}{k} \mathbf{q} = 0, \tag{3}$$

where P is the pressure, $\mathbf{g}$ is the gravity vector, k is the permeability of the medium and ρ and μ are the density and viscosity of the fluid.

Mass transport:
$$\epsilon \rho_T + \mathbf{q} . \nabla \rho = \nabla . (\boldsymbol{\kappa} . \nabla \rho). \tag{4}$$

Here ϵ is the porosity, $\boldsymbol{\kappa}$ is the diffusivity tensor and T is time.

It is convenient to take X and Y axes in the plane of an assumed initially horizontal interface, having the origin moving with the interface, and the z axis directed vertically upwards. Now, if there is a uniform constant superposed flow W_0 upwards, the velocity of the interface will be W_0/ϵ. If the flow vector $\mathbf{q}$ is now measured in this moving system, it is found that (2) to (4) are unchanged in form except that the left-hand side of (3) contains a resistance term $\mu W_0/k$ acting in the Z direction.

For the non-linear problem posed by the system when the wave amplitude is large, it will be assumed that the following decomposition of the density profile can be made. Let the density of the upper fluid be $\rho_0 + \Delta$, of the lower fluid $\rho_0 - \Delta$. Further, let $\bar{\rho}(Z, T)$ be the mean density over the X, Y plane at height Z (within the finger system) so that

$$\begin{aligned} \rho &= \{\rho(X, Y, Z, T) - \bar{\rho}(Z, T)\} + \{\bar{\rho}(Z, T) - \rho_0\} + \rho_0 \\ &= (\phi + \theta)\Delta + \rho_0, \end{aligned} \tag{5}$$

where $\phi(Z, T) = (\bar{\rho} - \rho_0)/\Delta$ and $\theta(X, Y, Z, T) = (\rho - \bar{\rho})/\Delta$ are dimensionless variables. Note that ϕ represents the variation of the mean density at height Z from the central value ρ_0, while θ represents point fluctuations of density relative to the mean value over the plane at the given value of Z.

Variation of viscosity μ with density will be represented approximately by the first two terms of a Taylor expansion

$$\mu \approx \mu_0 \{1 + (\Delta/\mu_0)(d\mu/d\rho)_0 (\phi + \theta)\}, \tag{6}$$

where the factor $(\Delta/\mu_0)(d\mu/d\rho)_0$ will be assumed small relative to unity. It is thus appropriate to apply the Boussinesq approximation with respect to μ.

In terms of the quantities defined above, let

$$\Lambda = \frac{kg\Delta}{\mu_0} + \frac{\Delta}{\mu_0} \left(\frac{d\mu}{d\rho}\right)_0 W_0 \tag{7}$$

be the characteristic velocity for miscible fluids, analogous to the parameter Λ^* given by (1) for the immiscible case. Then, if $(u, v, w) = \mathbf{q}/\Lambda$ is a dimensionless flow vector, eliminating the pressure from Darcy's law (3) gives

$$\nabla_1^2 \theta + \nabla^2 w = 0, \tag{8}$$

in which ∇_1^2 signifies $\partial^2/\partial X^2 + \partial^2/\partial Y^2$.

In the equation of mass transport, it is convenient to assume a simple form for the diffusivity tensor. Since the applied flow rate W_0 is directed normal to the interface, it will be assumed that there is a coefficient of longitudinal diffusion (combined with dispersion) κ_l in the direction of W_0, and a coefficient of transverse diffusion and dispersion κ_t ($\leqslant \kappa_l$) in any direction normal to the direction of W_0. Both of these coefficients will be taken to be at least approximately constant. Then the diffusion term can be simplified. If all the dependent variables are now represented by dimensionless quantities, (4) can be written

$$\phi_S + u\theta_X + v\theta_Y + w\theta_Z - \frac{\kappa_l}{\Lambda}\phi_{ZZ} + \theta_S + w\phi_Z - \frac{\kappa_t}{\Lambda}\nabla_1^2\theta - \frac{\kappa_l}{\Lambda}\theta_{ZZ} = 0, \tag{9}$$

where $S = \Lambda T/\epsilon$ is a length variable analogous to the amplitude of fingers growing between two immiscible fluids.

The equations (8) and (9), with the equation of continuity, could be replaced by difference equations for numerical solution, as done by Elder (1968) for two-dimensional flow. Here, however, a form of spatial averaging will be introduced (§ 3) in order to simplify the system. The experimental observations which assist in formulating this approach are described in § 2.

2. Experimental observations using Hele–Shaw cells

For visual studies on flow through porous media, the Hele–Shaw cell has been used by several workers, e.g. Saffman & Taylor (1958), Wooding (1963), Elder (1967). The analogy can be used for two-dimensional flows only.

Lamb (1932, § 330) has summarized the theory of Hele–Shaw flow for a homogeneous fluid. Let rectangular co-ordinates be taken in the plane of a cell sloping at an angle β to the horizontal, with the Z axis directed up the line of greatest slope and the X axis horizontal; the fluid velocity averaged across the space between the plates at a given point (X, Z) is

$$\mathbf{q} = -(h^2/12\mu)\,(\partial/\partial X, \partial/\partial Z)\,(P + g\rho Z\sin\beta), \tag{10}$$

where h is the spacing between the plates, P is the pressure, and $g\sin\beta$ is the gravity component in the plane of the cell. Then $h^2/12$ is the equivalent permeability.

When a Hele–Shaw cell is used to simulate the flow of non-homogeneous fluid in a porous medium, it is generally assumed that the variation in fluid properties is negligible over distances in the X, Z plane comparable with the plate spacing h. Experimental work with an analogue of the two-dimensional Schlichting jet (Wooding 1963) provides a check on the validity of this assumption. Measurements were made of the distance of advance (Z_m say) of the leading edge of a dense laminar 'starting plume' in a Hele–Shaw cell. If Darcy's law is obeyed, the velocities and density in the established part of the plume can be calculated from Schlichting's (1933) theory; in particular, the fluid velocity W_a on the axis of the plume is known. In this way it has been found that

$$dZ_m/dT = 0{\cdot}33W_a, \tag{11}$$

i.e. of a form expected from similarity provided that Schlichting's theory applies.

Experimental method

Two Hele–Shaw cells were constructed from sheets of $\frac{1}{4}$ in thick polished plate glass, having internal boundaries made from strips of rubber insulating tape impermeable to water flow. Figure 1 (*a*) shows the arrangement. Two boundaries parallel to the Z direction and separated by a known distance were attached permanently to one sheet of glass, and served also to control the spacing of the plates. A horizontal removable strip, passing through a slot cut in one permanent boundary, was used to divide the cell into equal upper and lower portions. The first (smaller) cell was not closed at the bottom, mainly in order to achieve satisfactory pressure equalization on the two sides of the removable boundary, but the second cell was closed as shown.

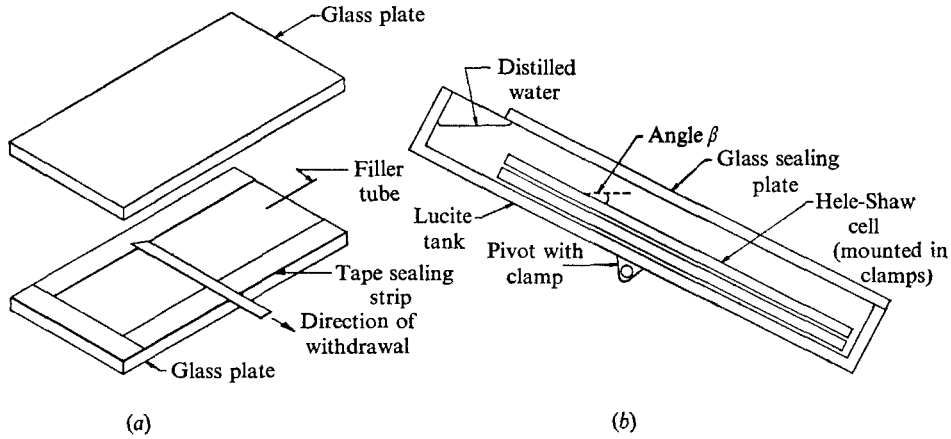

FIGURE 1. Hele–Shaw cell apparatus for producing an unstable diffusing interface. (*a*) Construction of cell. (*b*) Cell immersed in tilted tank.

Cell	I	II
Horizontal spacing of boundaries (cm)	12·0	25·45
Approximate total height (cm)	30	60
Mean plate spacing h (cm)	0·0351	0·0277
Equivalent permeability k (cm^2)	$1{\cdot}03 \times 10^{-4}$	$6{\cdot}39 \times 10^{-5}$
Width of central removable strip (cm)	0·63	1·27
Description of solute	Potassium permanganate	Potassium permanganate
Density of source solution relative to water at 18° C. ρ_s/ρ_w	1·0041	1·00695
Approximate diffusivity of source solution κ (cm^2/sec)	6×10^{-6}	6×10^{-6}

TABLE 1. Dimensions of two Hele–Shaw cells used for experimental work, and brief descriptions of source solutions. The value adopted for κ is from Fürth & Ullman (1926).

Table 1 gives the dimensions of the two cells. In addition to the differences in size, quite different values of permeability and solution density applied in the

two cases. For this reason, experiments using cell I have been included as useful comparisons, although the experiments with this cell were of a preliminary nature and were fairly rough.

Values of Λ for a cell tilted at angle β were calculated from the formula

$$\Lambda = \frac{\rho_s - \rho_w}{2} \frac{kg \sin \beta}{\mu} \tag{12}$$

based on (7), where ρ_s and ρ_w are densities of solution and water respectively, and k is the equivalent cell permeability given in table 1. The values of dynamic viscosity μ and density ρ_w were obtained from tables for water (Dorsey 1940) appropriate to the measured mean temperature in each experiment, the change of μ due to the presence of solute being assumed insignificant.

Initial filling of each cell was carried out by immersing both plates in distilled water in a transparent tiltable tank (figure 1(*b*), (*c*), plate 1) and then clamping the plates together with the removable strip in place. The upper half of the cell was filled with dilute potassium permanganate solution, using a fine glass capillary tube thin enough to pass between the plates and provide a source of fluid about 5 cm from the top of the cell. The strength of the source was adjusted to provide a broad two-dimensional plume (Wooding 1963) which consisted of a core of uniform undiluted solution bounded on either side by a mixing layer. As would be expected, the upper edge of the solution collecting above the removable strip consisted of dispersed fluid exhibiting a gradual change of density with height. However, this mixed zone was forced to the top of the cell during the filling process, away from the region of interest.

To initiate an experiment, the removable strip was withdrawn steadily to one side of the cell. Inevitably, removal of the strip left some space which had to be filled by movement of fluid into the cell; however, the motion was necessarily a Stokes flow because of the small spacing of the plates, and little mixing appeared to be induced at that stage. Some difficulty was encountered with the introduction of long wavelength disturbances (figure 2(*b*), plate 1), but the growth rate of these was insignificant in comparison with that of the most amplified disturbance.

Qualitative disturbances

The photographic sequence of figure 2(*a*), plate 2, shows the features generally recorded with the growth of waves at the unstable interface. After formation of the interface, some little time elapses before a large number of small waves appear. These grow rapidly, and the amplitude becomes greater than the wavelength. The waves have developed the character of fingers, resembling those described by Saffman & Taylor (1958) and Chuoke, van Meurs & van der Poel (1958).

Apparently, the number of fingers also diminishes with time. There is a tendency for adjacent waves to coalesce by mutual entrainment—a process controlled by diffusion—thus decreasing the apparent wave-number. Elder (1968) notes a similar effect which he calls the 'amalgamation of eddies'. The process of waves, or fingers, growing and slowly spreading results in considerable mutual interference; an irregular pattern is likely to result.

An additional complicating effect deserves mention. At an advanced stage of development of the fingers, the fronts tend to become unstable and break into two separate fingers (figure 2(*b*)). Thus the process of wave-number decrease ultimately could be arrested. A similar instability has been noted in connexion with the dense starting plume described earlier in this section, and appears to be associated with the increase in transverse length scale. This phenomenon is not treated in the present paper.

Experimental results

Because of the irregularities in the pattern of growing fingers, only statistical averages were extracted from the photographs. The mean wavelength was obtained by counting the total number of growing wave crests and troughs visible on each photograph, and dividing this number into twice the width of the cell. Elder (1968) used a similar method. Naturally, the estimate of the mean improves as the number of fingers increases, and the measurements using the larger cell (II) show appreciably less scatter than those with cell I. To measure the mean amplitude, or half-length of finger, an envelope was sketched around the pattern, touching the crests on one side and the troughs on the other, and the area measured with a planimeter. The condition $W_0 = 0$ was also checked approximately in a few cases, by area measurements of the uncoloured fluid, in cell II.

Summaries of the data measured from photographs of seven experiments, two of these in cell I and five in cell II, are plotted in figures 3 and 4 as mean wavelength *versus* time, and as mean amplitude versus ΛT respectively. A key to the plotting symbols is given in table 2. The table also shows that the experimental values of Λ covered a range of about 16 to 1. Detailed experimental measurements are given elsewhere (Wooding 1969).

Cell	Angle β (°)	$10^3\Lambda$ (cm/sec)	Temp. range (°C)	Symbol (figures 3, 4)
II	$2{\cdot}87 \pm 0{\cdot}05$	0·96	15·3–15·6	■
I	5·42	1·68	14·0–14·1	▲
II	5·75	1·88	14·3–15·0	◆
I	9·82	3·19	15·9–16·0	▼
II	11·5	3·85	15·5–15·6	⊕
II	24·5	7·72	14·6	⊗
II	55·9	15·8	16·5	●

TABLE 2. Summary of experimental parameters (see also table 1).

From figure 3, the mean wavelength measurements tend towards a line defined by

$$0{\cdot}0190T^{\frac{1}{2}} \approx 2\pi(\kappa T)^{\frac{1}{2}}/0{\cdot}827 \qquad (13)$$

in c.g.s. units, where the diffusivity value κ has been taken from table 1. It is worth noting that the mean wave-number is close to $(\kappa T)^{-\frac{1}{2}}$. Since, as will be shown later, longitudinal diffusion is not significant at large times, it seems likely that transverse diffusion is the controlling factor, giving an apparent wave-

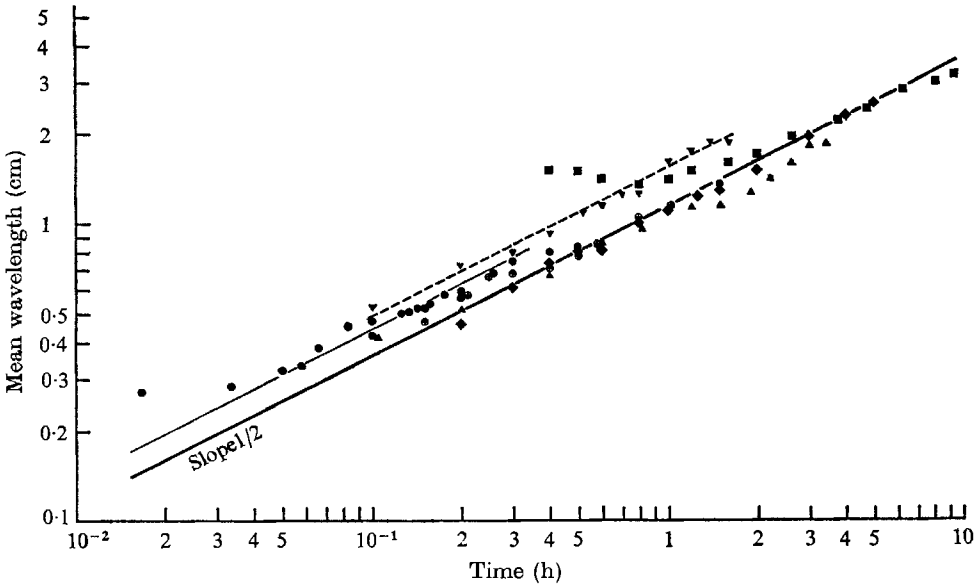

FIGURE 3. Mean wavelength *versus* time measured from seven experiments. Parameters are given in tables 1 and 2. ——, mean wavelength measured in $q = 1$ régime (cf. § 4); ——, mean wavelength calculated for $q = 2$ régime; – – – –, mean wavelength measured in one experiment using cell I, $\Lambda \approx 3{\cdot}19 \times 10^{-3}$ cm/sec.

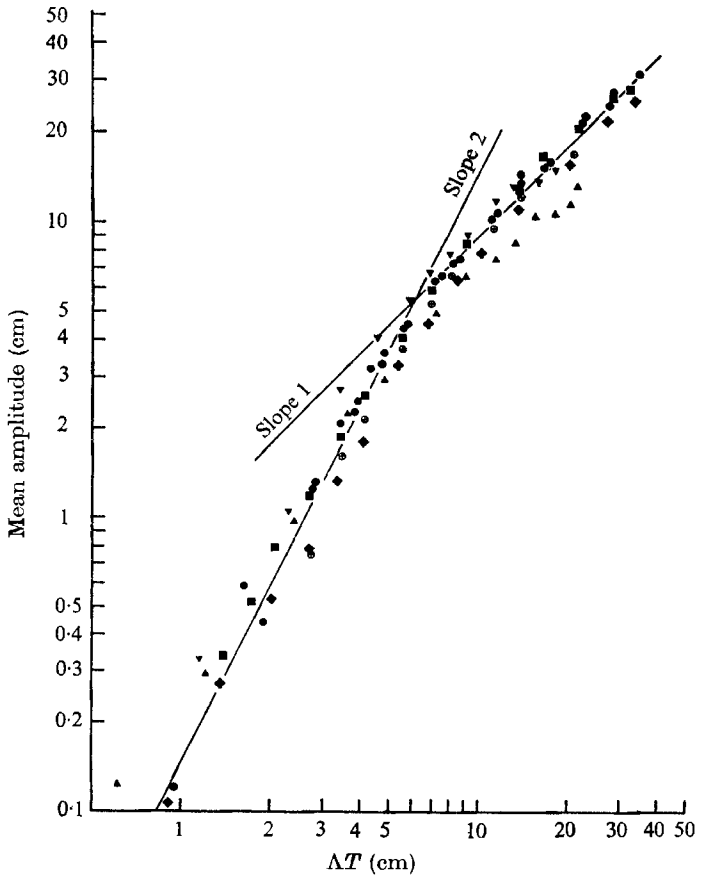

FIGURE 4. Mean crest trough amplitude *versus* $\Lambda T = S$ measured from seven experiments with parameters given in tables 1 and 2. Straight lines fitted to data from five experiments using cell II represent $q = 2$ and $q = 1$ régimes (§ 4).

number which decreases steadily due to the decay or entrainment of high wave-number fingers.

One set of experimental results, indicated by the broken line in figure 3, lies entirely above the main line. This experiment was carried out in Hele–Shaw cell I which was open at both ends, and an appreciable convective flow was taking place through the cell due to the excess density of the solution. The calculated longitudinal dispersion using Taylor's (1953) theory (see also Wooding 1960) was found to be roughly three times the molecular diffusivity, which could increase the growth rate of interface thickness and so reduce the wave-number of the most-amplified initial disturbance (cf. Elder 1968). Note that significant longitudinal dispersion was also present in cell II for large Λ, due to the rapid growth rate of the fingers. However, the modification to the wave-number appeared to be small in this case, indicating that the 'selection' of the dominant disturbance had occurred at an early time when velocities were small.

Most of the points measured at early stages of the experiments lie above the heavy full line in figure 3. From the previous paragraph, these points indicate the possible existence of an early régime of relatively low wave-number, rather than a dispersion effect.

As figure 4 shows, the experimental results for mean amplitude fall close to a pair of straight lines on a double-log plot with ΛT in the abscissa.

$$Z_m = 0{\cdot}0732S^2 \quad (S < 6{\cdot}1\,\text{cm}) \tag{14}$$

and

$$Z_m = 0{\cdot}446S \quad (S > 6{\cdot}1\,\text{cm}), \tag{15}$$

where Z_m is one-half of the crest-trough amplitude in cm. It is apparent that the effect of diffusivity changes upon amplitude is quite small (cf. Slobod & Thomas 1963). This is consistent with the form of equation (9). If longitudinal dispersion is neglected, as described in § 3, a change in Λ affects only the transverse diffusion term, and the main consequence is the change of wave-number. It follows that the amplitude depends principally upon the variable S.

From (14), it appears that the experimental results overlap the final phase (3 in § 1) of Elder's numerical experiments.

The second relation (15) is particularly interesting since the miscible fluid fingers appear to grow at less than one-half of the growth rate of fingers between immiscible fluids. A likely explanation is that the density distribution across a finger resembles a diffusion profile, as would be expected if transverse diffusion and associated fluid entrainment were taking place.

3. Approximate equations for finger growth

A detailed analysis of the growth problem is not attempted in this paper, but some of the observed average properties of large amplitude fingers may be derived from the equations (2), (8) and (9) of § 1. It will be noted that only (9) is non-linear, and that the equation involves two weakly-coupled parts, the first five terms being nearly aperiodic in the X, Y plane (i.e. composed largely of contributions dependent upon only Z and S), while the remaining four terms are quasi-periodic in these variables.

For large S, the ratio of terms involving ϕ_{ZZ} and ϕ_S respectively in (11) is $O(\kappa_l S/\Lambda Z^2)$. Hence, if the typical Z scale increases more rapidly than $S^{\frac{1}{2}}$, as the experimental results show, then the term in ϕ_{ZZ} may be neglected for large S. A consideration of numerical values appropriate to the experimental work indicates that this approximation could be assumed valid for all of the recorded measurements. An argument similar to the above applies also to the term involving θ_{ZZ}. In (8), the situation is a little different; from experiment the typical scale in the X, Y plane does not increase more rapidly than $S^{\frac{1}{2}}$, and w_{ZZ} ultimately becomes negligible relative to $\nabla_1^2 w$. Then (8) can be integrated to give

$$\theta + w = 0. \tag{16}$$

Equations governing averaged quantities

Now suppose that the saturated medium is bounded by a cylindrical container of arbitrary cross section with vertical impermeable walls. The wall boundary conditions are that the normal components of velocity and θ gradient vanish; but, if it is also assumed that the cross-sectional area is large enough to contain many fingers, the influence of the sidewalls upon quantities such as horizontal wave-number will be small. When (16) is used to eliminate θ from (9), and the latter equation is averaged over the entire cross section at a given value of Z, the result is

$$\phi_S = \overline{w_Z^2}. \tag{17}$$

Again, let (9) be multiplied by $w/(\overline{w^2})^{\frac{1}{2}}$ and the average taken over the same cross section, to give

$$(\overline{w^2})_S^{\frac{1}{2}} = (\overline{w^2})^{\frac{1}{2}} \left(\phi_Z - \frac{\kappa_l}{\Lambda}\alpha^2(Z,S)\right) - \tfrac{1}{2}\overline{w_Z^3}/(\overline{w^2})^{\frac{1}{2}}, \tag{18}$$

where the slowly-varying function α is an 'equivalent mean wave-number', defined by

$$\alpha^2 \overline{w^2} = \overline{w_X^2} + \overline{w_Y^2}. \tag{19}$$

A necessary assumption is that the observed mean wave-number (§ 2) does not differ greatly from this quantity. In (18), the term involving $\overline{w_Z^3}$ will be neglected. If (9) is multiplied by w^2 and averaged as before, the growth rate of $\overline{w^3}$ is found to depend primarily upon the small quantity $\{\frac{3}{2}(\overline{w^2})^2 - \overline{w^4}\}_Z$ which, in fact, is zero for w sinusoidal. Also $\overline{w^3}$ is expected to be small from the nearly symmetrical properties of the flow.

Equations corresponding to (17) and (18) have been derived for the problem of flow in a vertical tube filled with saturated porous material (Wooding 1962). In that case, a fairly satisfactory approximation was made for the transverse density distribution from the geometry of the tube cross section, leading to an estimate for the dominant wave-number. Such information does not exist in the present case since the boundary conditions are assumed to be unrestricting. An equation involving α_S can be derived by multiplying (9) by $\nabla_1^2 w$ and averaging over X and Y to give

$$\alpha_S = \frac{\kappa_l}{\Lambda\alpha}(\alpha^4 - \overline{(\nabla_1^2 w)^2}/\overline{w^2}) \tag{20}$$

and $\alpha_S \leqslant 0$ from (19) and (20) using the Schwartz inequality. Continuation of the averaging process to obtain an equation for $\overline{(\nabla_1^2 w)^2}$, and so on, evidently leads to an unclosed set of equations. In this paper (§ 4), a closed system is obtained by assuming a form for α^2 in (18) based upon similarity considerations.

Characteristic form and jump conditions

As already observed (Wooding 1962), the differential equations (17) and (18) form a hyperbolic system, and the possibility exists of discontinuities arising in ϕ and $\overline{w^2}$. In characteristic form the equations can be written

$$dZ/dS = \pm (2\overline{w^2})^{\frac{1}{2}}, \tag{21}$$

$$\frac{d}{dZ}(\phi \mp (2\overline{w^2})^{\frac{1}{2}}) = \frac{\kappa_l}{\Lambda}\alpha^2(Z, S), \tag{22}$$

the upper signs referring to ascending characteristics and the lower signs to descending characteristics.

In the present problem it is necessary to suppose that the fronts of all ascending fingers (say) fall within a fairly narrow zone centred at $Z_m(S)$, and to replace this zone by a discontinuity. Let ϕ_0 denote the dimensionless density just ahead of the advancing fingers and assume that $\overline{w_0^2} = 0$ there, i.e. that the fluid is not in motion. Let the suffix m now refer to any quantity measured just behind the jump. If (17) and (18) are each integrated over a short interval in Z which contains the zone centred at Z_m, the two following jump conditions result.

$$dZ_m/dS = U(S) = \tfrac{2}{3}\{\phi_0(S) - \phi_m\} = \pm (\tfrac{2}{3}\overline{w_m^2})^{\frac{1}{2}}, \tag{23}$$

where U is the jump velocity, and the $\pm$ signs on the right have been added to include both ascending and descending jumps.

Non-invariance of the averaged equations

Lax (1954) was the first to point out that the 'weak' solutions associated with a given non-linear hyperbolic system depend upon the form in which the equations are written. Owing to the presence of discontinuities the above system is not Lipschitz continuous, and its solution will be non-invariant in that way; e.g. if the weight function $w/(\overline{w^2})^{\frac{1}{2}}$ is replaced by w (equivalent to a non-linear transformation of (18)), the differential equation is effectively unchanged but a new set of jump conditions and new solution result. Generally, only one solution is physically appropriate. Since (18) is not a 'standard' conservation law, its correct form is not clear *a priori*. However, subsequent comparison of the experimental results with numerical solutions of (17) and (18), subject to (23), appear to show that the chosen formulation is physically correct.

4. Similarity solutions

The power law growth of finger amplitude observed experimentally suggests that the more obvious features of the system might be modelled by similarity solutions of relatively simple form. Let

$$\zeta = L^{q-1}Z/S^q, \quad \phi = (S/L)^{q-1}F(\zeta), \quad (2\overline{w^2})^{\frac{1}{2}} = (S/L)^{q-1}G(\zeta), \tag{24}$$

where L is a length scale and q an exponent, both at present unspecified. Then (17) and (18) become a pair of simultaneous ordinary differential equations.

$$q\zeta F' + GG' = (q-1)F, \tag{25}$$

$$GF' + q\zeta G' = (q-1+\gamma)G, \tag{26}$$

in which

$$\gamma(Z,S) = (\kappa_t/\Lambda)S\alpha^2(Z,S), \tag{27}$$

and $(\,)'$ signifies $d/d\zeta$. The S dependence of α^2 is not known *a priori*; however, for (25) and (26) to be independent of S it is necessary either (i) that γ should be negligible, or (ii) that γ should be independent of S. Case (i) is probably not of direct interest here because it can only hold for waves which, from § 1, would have very slow rates of initial growth. In any event γ must ultimately become significant for large enough S. If a power law growth then appears, (ii) must apply and $\alpha \propto S^{-\frac{1}{2}}$, in accordance with the experimental observations.

An additional complication arises from the unknown ζ dependence of α^2, and hence of γ. However, the main solution properties are unlikely to be greatly affected by slow variations from this source which will, therefore, be neglected.

In terms of the new variables defined in (24), the jump conditions (23) become

$$q\zeta_m = \tfrac{2}{3}(F_0 - F_m) = \pm 3^{-\frac{1}{2}}G_m, \tag{28}$$

where

$$F_0 = (L/S)^{q-1}\phi_0(S). \tag{29}$$

Since F_0 must be independent of S, it is evident that $\phi_0 \propto S^{q-1}$; if the power law dependence of ϕ_0 upon S is known, q may be determined, or *vice versa*. Also, as $\zeta = \zeta_m =$ constant at the jump, (24) gives $Z_m \propto S^q$ for the growth rate of amplitude. The experimental results of figure 4 indicate the existence of a flow régime with $q \approx 2$ followed by a régime for which $q \approx 1$. A finite transition zone probably separates these two power law régimes.

Similarity properties when $q = 1$

For the case of fingers advancing into homogeneous still fluid, $\phi_0(S) = 1$ in (29) so that $q = 1$, $F_0 = 1$ and the unknown length L disappears. Then F can be eliminated from (25) and (26) to give

$$G' = -\gamma/(G/\zeta - \zeta/G). \tag{30}$$

The appropriate solution of (30) is

$$\begin{aligned} F/C_1 &= \tfrac{1}{2}\gamma\int_0^t t^{-\frac{1}{2}}\{1+(\gamma-1)t\}^{(2-3\gamma)/(2\gamma-2)}\,dt, \\ G/C_1 &= \{1+(\gamma-1)t\}^{-\gamma/(2\gamma-2)}, \end{aligned} \tag{31}$$

where the parameter

$$t = \zeta^2/G^2. \tag{32}$$

Here F and G are odd and even functions of ζ respectively. The constant $C_1(\gamma)$ of integration appears as a scale factor because of homogeneity in the ratios $F:G:\zeta$. Solution curves of F/C_1 and G/C_1, taking positive ζ/C_1 as abscissa, are given in figure 5 (*a*) for selected values of the parameter γ. Note that the solution (31) simplifies at particular values of γ. For example, when $\gamma = \frac{2}{3}$, then

$F/C_1 = 2\zeta/3G$ and $G/C_1 = 1-\zeta^2/3G^2$ and the numerical values fall within about 1 % of the experimental results.

Figure 5 (*a*) can be used to obtain a graphical solution of the system (31) and (32) subject to the discontinuity conditions (28). Four relations are available for the five quantities γ, C_1, F_m, G_m and ζ_m; the problem could be rendered unique if either γ or ζ_m were known from appropriate initial conditions. In figure 6 the dependence of F_m, G_m and $\gamma = \gamma_1$ upon ζ_m is shown. A single point—a mean result from the five experiments using cell II described in § 2, and representing the observed values of γ_1 and ζ_m—falls on the γ_1 curve.

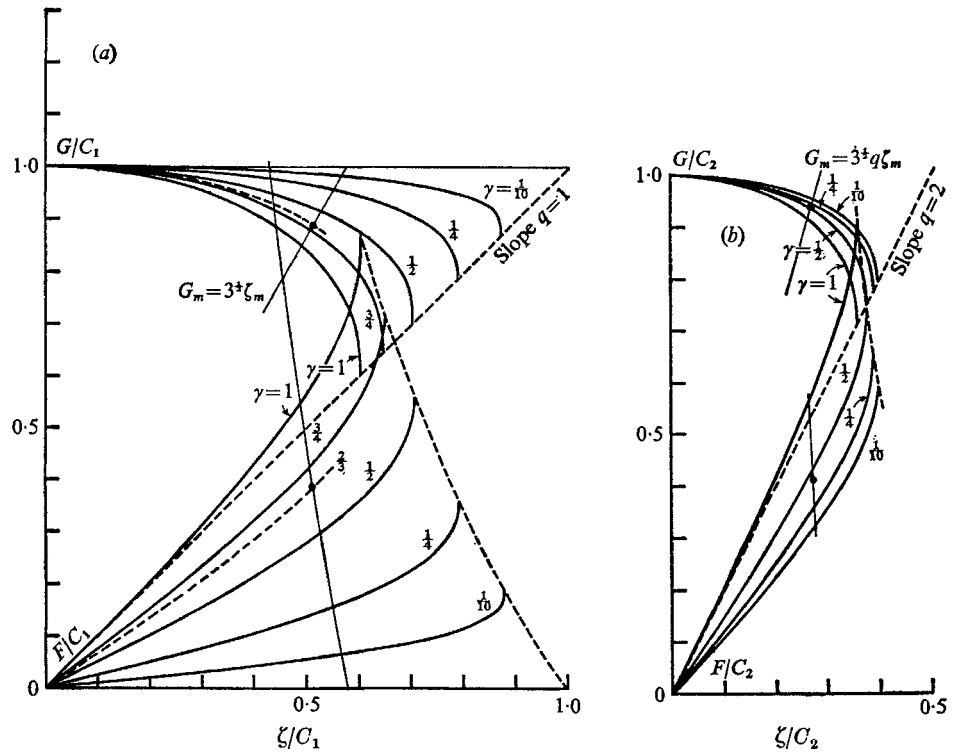

FIGURE 5. Solution curves of equations (25) and (26) for similarity variables F/C and G/C *versus* ζ/C. ——, jump condition (28) relating ζ_m to G_m and corresponding values of F_m. (A second condition from (28) involving $F_0 - F_m$ (not shown) sets C.) – – –, locus of maxima of ζ which, by jump conditions, fall outside physical range. ●, experimental values. (*a*) $q = 1$, $C = C_1(\gamma)$; (*b*) $q = 2$, $C = C_2(\gamma)$.

In general, ζ_m decreases as the mean wave-number is increased, since a greater mean density gradient is needed to maintain steady flow at higher wave-numbers. From (18), the steady flow condition is $\phi_Z = (\kappa_t/\Lambda)\alpha^2(Z, S)$, and this is formally identical to the criterion for neutral stability of a Fourier component of arbitrary amplitude with horizontal wave-number α and zero vertical wave-number. In similarity variables the condition is $F' = \gamma$, which also satisfies the problem as $\zeta \to 0$. That is, the mean density gradient at the centre of the fingers when $q = 1$ corresponds to the neutral value. It is also the point of minimum gradient.

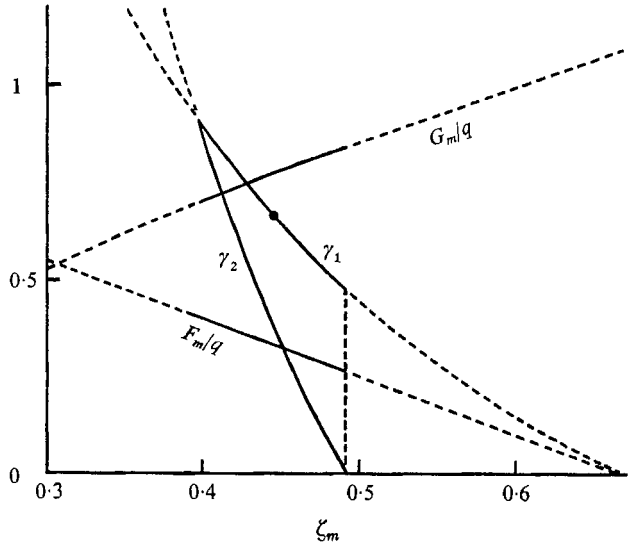

FIGURE 6. F_m/q, G_m/q and γ_q, where $q = 1, 2$, as functions of ζ_m. By definition ζ_m has the same value for both régimes, so that γ undergoes a transition $\gamma_2 \to \gamma_1$.

Similarity properties when $q = 2$

For this flow régime, Elder (1968) proposed a physical model (3 in § 1) in which acceleration continues while fluid from the diffusion layer is being drawn into the fingers, thus progressively increasing the effective density difference. The implication is that $\phi_0(S)$ increases with S, but does not further specify its form. Since $q \approx 2$ from experiment, (29) gives $\phi_0 \propto S$ over a finite range of S. Therefore, assume the approximate representation

$$\begin{aligned} \phi_0(S) &= \pm S/L' \quad (S \leqslant L'), \\ &= \pm 1 \quad\quad (S > L'), \end{aligned} \tag{33}$$

the sign depending upon the direction of motion of the discontinuity. Here L' is a further length parameter.

The quantity ζ_m corresponds to the location of the discontinuity, and its value may be taken constant through both the $q = 2$ and $q = 1$ régimes of flow. Then, in (24), let L be taken equal to the value of S (= 6·1 cm) at which the two experimental curves (14) and (15) intersect. It follows at once from the discontinuity conditions (28) that $(F_0 - F_m)/q$ and G_m/q are unchanged when q changes, so that both $F_0 - F_m$ and G_m decrease by a factor of 2 at $S = L$. This corresponds to the difference in slope of the lines (14) and (15) at the point of intersection in figure 4.

For $q = 2$, the quantities F/C_2 and G/C_2 have been obtained as functions of ζ/C_2 by numerical integration of equations (25) and (26) (figure 5(*b*)), where $C_2(\gamma)$ is a new scaling constant. A graphical fit of the jump conditions (28) to this solution gives $F_0 = 2$, and (29) and (33) give $L = 2L'$. Thus C_2 and γ can be determined as functions of ζ_m.

The dependence of $\gamma = \gamma_2$ as well as F_m/q and G_m/q upon ζ_m for $q = 2$ is shown in figure 6. This indicates that γ is smaller when $q = 2$ than when $q = 1$ in the

relevant range of ζ_m. In fact, if $\zeta_m \approx \frac{4}{9}$, $\gamma_2 \approx 0{\cdot}40$, corresponding to a mean wave-number about 0·8 times that observed for the case $q = 1$. This result is in fair agreement with measurements made at early stages in most experiments (figure 3).

Transition régime

The observed increase in γ, when q decreases from 2 to 1, appears reasonable provided that the transition between the two régimes is characterized by a reduced rate of decrease of the wave-number in the physical X, Y plane, and if S at least doubles during the transition. Little can be deduced from similarity considerations, and the transition is examined in more detail numerically (§ 5).

5. Numerical solution of the averaged equations

For a solution using a high-speed digital computer, the system of hyperbolic equations (17) and (18), subject to jump conditions (23), is generally preferable to the characteristic form (21) and (22).

Let the equations be rendered fully non-dimensional by putting

$$s = S/L', \quad z = Z/L', \quad A^2(s) = \kappa_t \alpha^2 L'/\Lambda \tag{34}$$

and for convenience let $w' = (2\overline{w^2})^{\frac{1}{2}}$. Equations (17) and (18) become

$$\phi_s = \tfrac{1}{2}(w'^2)_z, \tag{35}$$

$$(\log w')_s = \phi_z - A^2(s), \tag{36}$$

the form of (36) being the most suitable one for a finite difference scheme (Fox 1962).

Instead of applying two sets of conditions at the jumps located symmetrically with respect to $z = 0$, it is more economical to consider one-half of the flow field, say for $z \geqslant 0$, and to apply a symmetry condition on the axis. Then, from (23) and (33),

$$\frac{dz_m}{ds} = U(s) = \tfrac{2}{3}\{\phi_0(s) - \phi_m\} = 3^{-\frac{1}{2}} w'_m, \tag{37}$$

at $z = z_m$, where

$$\begin{aligned} \phi_0(s) &= s \quad (0 < s \leqslant 1), \\ &= 1 \quad (s > 1). \end{aligned} \tag{38}$$

On $z = 0$,

$$\phi = w'_z = 0. \tag{39}$$

Finite-difference method

An efficient forward differencing scheme is due to Lax (1954). Its use is described in detail by Keller, Levine & Whitham (1960) and by Fox (1962). The particular form of time difference chosen by Lax to stabilize the equations introduces a small artificial diffusion term with coefficient $(\Delta z)^2/2\Delta s$, where Δs and Δz are the step lengths. The mesh size and ratio $\Delta s/\Delta z$ must be chosen so that the diffusion coefficient is small; otherwise the solution drifts into error although there is adequate stability. A linearized analysis of the non-linear finite difference equations gives the usual stability criterion

$$\Delta s/\Delta z \leqslant 1/w', \tag{40}$$

which, from (21), corresponds also to the Courant condition. It has been found by trial that a square mesh $\Delta s = \Delta z$ is appropriate. For a fixed step length, advancing in s is equivalent to refining the mesh (Lax 1954).

To solve the equations at the advancing jump, an additional relation is needed between the quantities at the jump (Fox 1962). Keller, Levine & Whitham achieve this by differentiating the jump velocity with respect to time. With this method, (37) gives two alternative formulae; that adopted here is

$$3\tfrac{1}{2}\frac{dU}{dS} = \frac{dw'_m}{ds} = w'_m\{(\phi_z)_m - A^2(s)\} + U(w'_z)_m \tag{41}$$

using (36). Again, following the above authors, the equations at the jump are replaced by an implicit difference scheme using backward s differences which is unconditionally stable; this is solved by iteration. Details of the method are given by Wooding (1969).

The initial conditions can be chosen from similarity considerations. A small starting value of s is taken so that the first values fall within the $q = 2$ régime, and corresponding values of ζ_m and γ_2 are obtained from figure 6. Then

$$z_m = \zeta^*_m s^2, \quad U = 2\zeta^*_m s, \tag{42}$$

where $\zeta^*_m = \zeta_m L'/L$. Starting values of ϕ_m and w'_m are calculated from (37), and approximate values of ϕ and w' at the intermediate mesh points are found by linear interpolation from ϕ_m and w'_m using (39).

A plausible form for $A^2(s)$ is based on similarity. Let $A^2 = \gamma_2/s$ for $s < 1$, i.e. for the duration of the $q = 2$ régime. Presumably the behaviour of A^2 will change at $s = 1$ when $\phi_0(s)$ changes according to (38), and A^2 will begin to decrease at a slower rate. The final form must be $A^2 = \gamma_1/s$ for $s \gg 1$, where γ_1 ($> \gamma_2$) is chosen from figure 6 at the given ζ_m. Two simple alternative assumptions will be made for the transition of A^2 between these two forms. Both involve taking A^2 constant. In the first case it is assumed that the transition begins at $s = 1$, and in the second at $s = 2$ (1 and 2 respectively in figure 7). Most of the actual transition probably lies within the area bounded by these two assumptions.

Although the numerical method does not trace characteristics, it is useful to map the backward characteristic (Γ_- in figure 7) from $z = z_m$ at $s = 1$, since this separates the $q = 2$ and transition régimes. At $z = 0$ the characteristic crosses a mirror image characteristic (Γ_+) which has started from the opposite jump at the same value of s; the second characteristic then separates the transition from the region in which the $q = 1$ régime is established. These two characteristics are traced numerically using (21).

Numerical results

Figure 7 shows the two finite difference solutions with parameter values close to the experimental values, for the two above assumptions concerning the wave-number transition. The similarity solutions are shown as broken lines.

In the $q = 2$ régime, the numerical solutions follow the similarity solutions quite closely, except for a small wavelike perturbation which possibly arises from the starting conditions. At $s = 1$ the rate of increase in w'_m is suddenly reduced, due to the fact that ϕ_0 has become constant. However, w'_m continues to

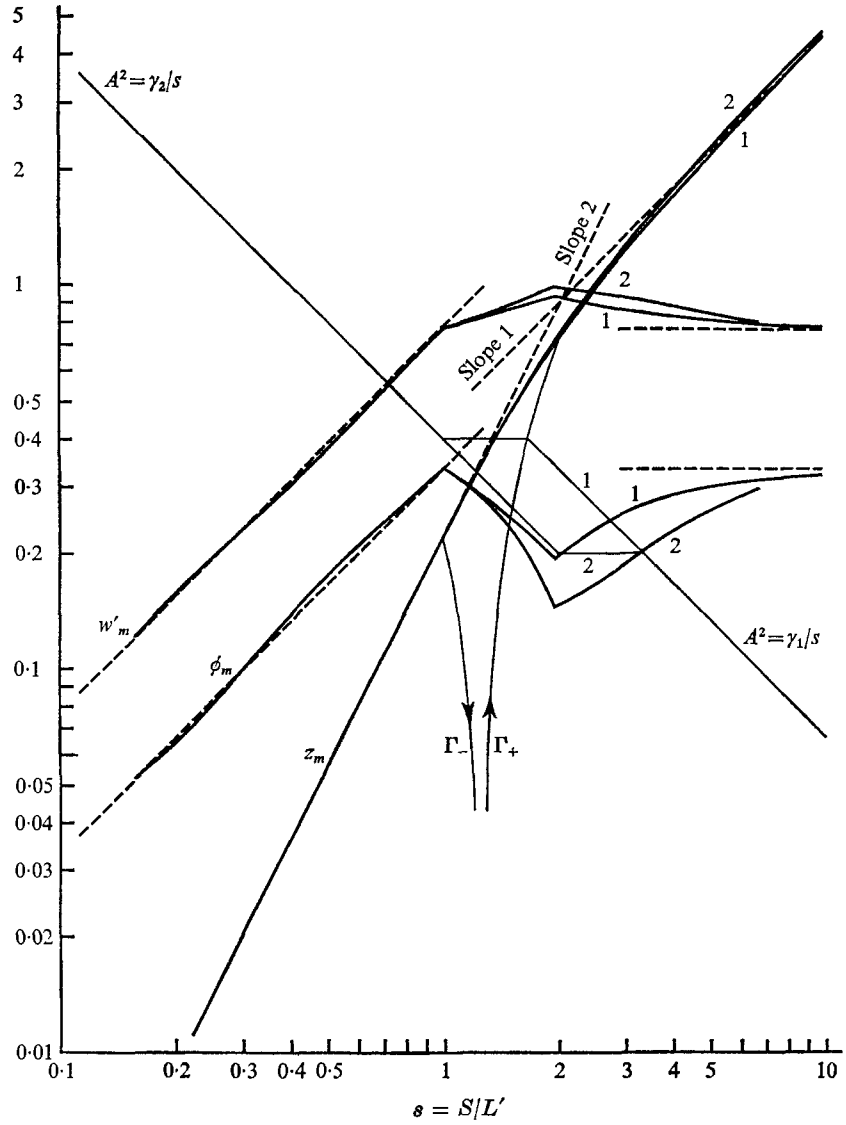

FIGURE 7. Finite difference solutions of equations (35) and (36), subject to conditions (37) to (39). ----, similarity solutions. Numerals 1, 2: alternative assumptions for transition of γ. $\Gamma_\pm$: ascending and descending characteristics which originate at start of transition. Parameter values: $\zeta_m = 0{\cdot}444$, $\gamma_1 = 0{\cdot}667$, $\gamma_2 = 0{\cdot}400$, $L' = \frac{1}{2}L = 3{\cdot}05$ cm.

increase because the advancing fingers contribute to the density difference; this contribution ceases only with the arrival of the second separating characteristic, which occurs at about $s = 2$. The decrease of ϕ_m for $1 < s < 2$ is a consequence of (37) and the constancy of ϕ_0. For $s > 2$ a readjustment occurs with w'_m decreasing slightly. There is little doubt that the numerical solution finally tends to the similarity solution for $q = 1$. The solution for z_m *versus* s follows similarity values very closely except in the transition region.

Figure 7 also illustrates changes of amplitude when the assumed form of the wave-number function A^2 is changed. The qualitative character of the solution is clearly unaffected, and the variation in z_m is probably too small to be detected experimentally.

6. Conclusions

At first glance, the apparent decrease of mean wave-number with time is surprising. However, an increase in scale is observed at the nose of a starting plume in a porous medium (§ 2) because the scale of the jet-like flow behind the nose increases as $(\kappa T)^{\frac{1}{2}}$. In the present problem, the experimental evidence shows that the mean wavelength increases approximately as $(\kappa T)^{\frac{1}{2}}$, but the fingers are so closely spaced that a scale increase is not possible without changes in the flow structure. A process of mutual entrainment may exist, the rate being controlled by diffusion, with the smaller fingers generally being absorbed by the larger.

The properties of the similarity solution with $q = 1$ indicate that a condition of near-neutral equilibrium is maintained as the fingers grow. Near the finger fronts, density gradients exceed the neutral value and a further instability can occur, resembling that described by Saffman & Taylor for a sharp interface. If the growth rate of this instability becomes important relative to the established finger growth rate, the equilibrium régime could be significantly modified. This did not appear to be the case in the experimental range considered.

Elder's suggestion—that acceleration continues while fluid from the diffusion layer is being drained into the fingers—provides a model which fits the observations satisfactorily. The process is not understood quantitatively for either L' or L to be calculated, but for the simplified model (33) the ratio $L/L' = 2$ appears to be established, and L can be measured. In the experiments described in § 2, $L' \approx 3$ cm, and uniform fluid begins to enter the finger system when $Z_m \approx 0{\cdot}65$ cm. That is, the finger amplitude at the start of the transition is quite small.

The analytical work was supported primarily by Grant no. 16000DGY, Federal Water Pollution Control Administration (U.S.A.), during the author's temporary research appointment at the California Institute of Technology (W. M. Keck Laboratory of Hydraulics and Water Resources). Experimental work was performed at C.S.I.R.O. Numerical computations described in § 5 were performed on the C.S.I.R.O. CDC 3600 computer.

REFERENCES

Chuoke, R. L., Van Meurs, P. & Van der Poel, C. 1959 *J. Petrol. Tech.* **11**, 64.

Dorsey, N. E. 1940 *Properties of Ordinary Water-Substance.* New York: Reinhold.

Elder, J. W. 1967 *J. Fluid Mech.* **27**, 609.

Elder, J. W. 1968 *J. Fluid Mech.* **32**, 69.

Foster, T. D. 1968 *Phys. Fluids*, **11**, 1257.

Fox, L. 1962 *Numerical Solution of Ordinary and Partial Differential Equations.* Oxford: Pergamon.

FÜRTH, R. & ULLMAN, E. 1926 *Kolloidschr.* **41**, 307.
HELLER, J. P. 1966 *J. Appl. Phys.* **37**, 1566.
HORTON, C. W. & ROGERS, F. T. 1945 *J. Appl. Phys.* **16**, 367.
KELLER, H. B., LEVINE, D. A. & WHITHAM, G. B. 1960 *J. Fluid Mech.* **7**, 302.
LAMB, H. 1932 *Hydrodynamics*, 6th ed. Cambridge University Press.
LAPWOOD, E. R. 1948 *Proc. Camb. Phil. Soc.* **44**, 508.
LAX, P. D. 1954 *Comm. Pure Appl. Math.* **7**, 159.
SAFFMAN, P. G. & TAYLOR, G. I. 1958 *Proc. Roy. Soc.* A **245**, 312.
SCHLICHTING, H. 1933 *Z. angew. Math. Mech.* **13**, 260.
SLOBOD, R. L. & THOMAS, R. A. 1963 *J. soc. Petrol. Engrs.* **228**, 9.
TAYLOR, G. I. 1950 *Proc. Roy. Soc.* A **201**, 192.
TAYLOR, G. I. 1953 *Proc. Roy. Soc.* A **219**, 186.
WOODING, R. A. 1960 *J. Fluid Mech.* **7**, 501.
WOODING, R. A. 1962 *J. Fluid Mech.* **13**, 129.
WOODING, R. A. 1963 *J. Fluid Mech.* **15**, 527.
WOODING, R. A. 1969 *Calif. Inst. of Technology Tech. Memo.* no. 69-5.

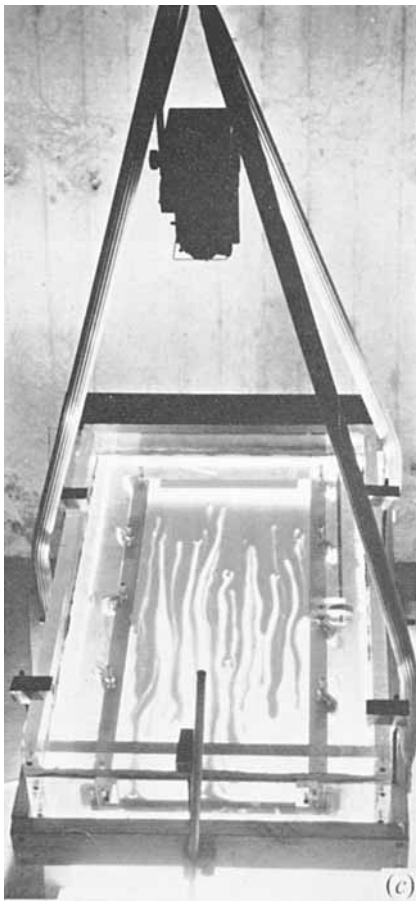

FIGURE 1(*c*). General view of Hele-Shaw apparatus.

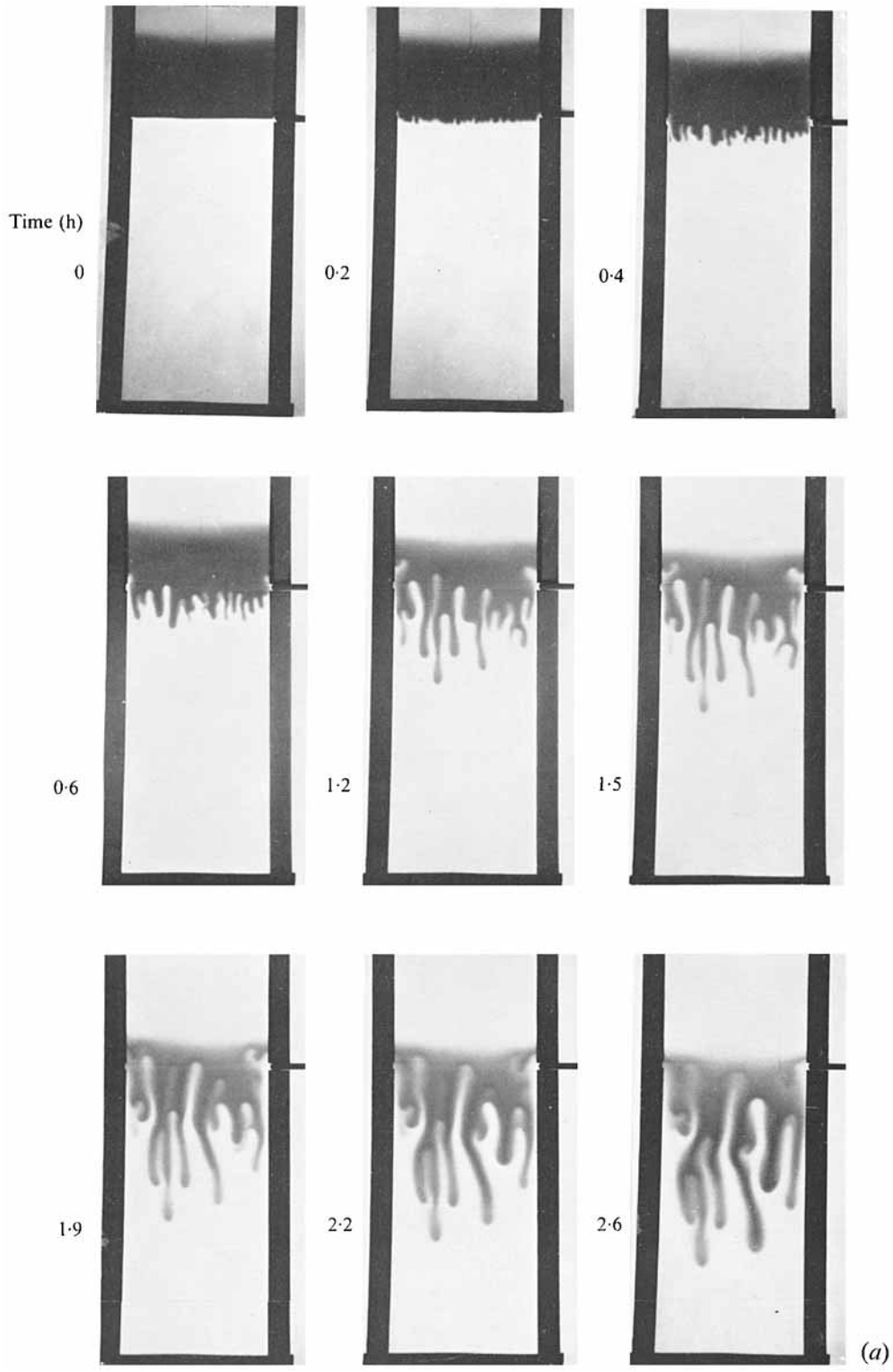

FIGURE 2(*a*). Growth of fingers in cell I; A $\approx 1{\cdot}68 \times 10^{-3}$ cm/sec.

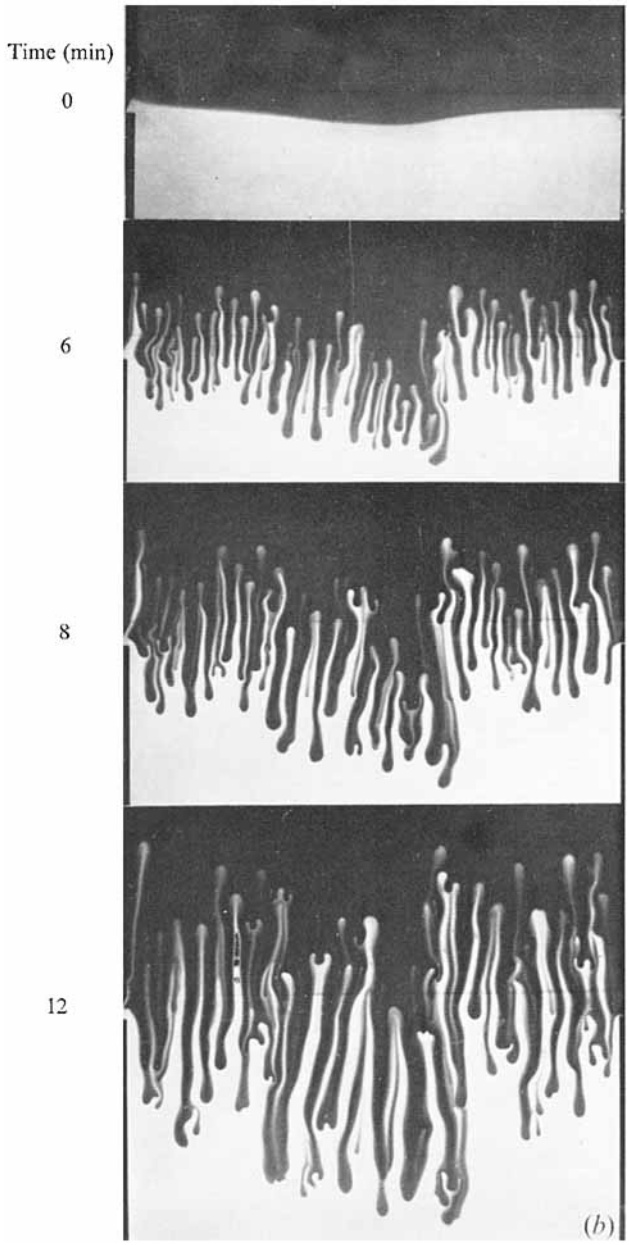

FIGURE 2(*b*). Break-up of finger fronts due to instability in cell II; $\Lambda \approx 15{\cdot}8 \times 10^{-3}$ cm/sec. An initial long wave disturbance which occurred at the interface in this experiment grew very slowly, and apparently did not affect the dominant wave growth.